MORE ON THE SECONDARY PENETRATION OF LONG RODS

Z. ROSENBERG and E. DEKEL

RAFAEL, P.O. Box 2250, Haifa, Israel

Abstract—The secondary penetration of long rods, impacting semi-infinite metallic targets, has been investigated since the early 60's, both experimentally and analytically. Several models have been proposed for the extra penetration which is achieved by these rods at the later stages of the process. However, the models are of limited applicability since they cover only limited regimes of the relevant parameters. In order to further understand the phenomenon of secondary penetration, we performed a large number of numerical simulations using the PISCES 2 DELK code. These simulations dealt with the relevant parameters in large ranges of variability, such as: the rod impact velocity, its aspect ratio (L/D), as well as the densities and strengths of rod and target material. We show that the semi-empirical formulations do not account for the whole range of these parameters. Our simulations show that the strength of the rod has a major influence on the values of the secondary penetrations. In addition, these values are strongly dependent on L/D and target strength. © 2001 Elsevier Science Ltd. All rights reserved.

INTRODUCTION

The penetration of long-rod penetrators into semi-infinite metallic targets, has been the focus of intense research for the past 40 years, as both armor and warheads are being improved by their designers. The complex process of normal penetration has been dealt with both by numerical simulations and analytical models, as well as with scaled and full-scaled experiments. One of the characteristic features of this process, especially at hypervelocity impacts, is that of the secondary penetration, which was first defined in [1]. This is the extra penetration caused by the expansion of the crater wall, after the completion of rod erosion, due to the finite energy imparted to the crater. This extra penetration was attributed by Christman and Gehring [1] to the last portion of the penetrator (with a length of one diameter), while the rest of the rod is assumed to perform the well-known primary (hydrodynamic) penetration. A simple empirical relation is given in [1], to account for the total penetration, which seems to account for a large number of data for rods with aspect ratios of 3-25 impacting aluminum and steel targets at 1-6 km/s (see [1]). Another mechanism for a secondary penetration has been suggested by Allen and Rogers [2], who observed a kink in their penetration curve for gold rods impacting aluminum targets. This kink, at about 2 km/s, was attributed to an enhanced penetration caused by the inverted rod. A simple analysis shows that for large penetrator to target density ratios, the inverted rod should be able to perform this extra penetration after the completion of rod erosion. Several workers adopted this mechanism for a possible interpretation of their data for metallic as well as ceramic targets (see [3]-[5]). However, in a recent work [6], we showed that the data of Allen and Rogers [2] for the gold rod is probably flawed by early release effects due to insufficient target thickness. Thus, the only valid mechanism for secondary penetration, which is also called the "after-flow", seems to be that of Christman and Gehring [1], which has also been investigated by Cullis and Nash [7], using 2D numerical simulations. Tate [8] treated the "after-flow" phase in ductile targets with an analytical model in which the target resistance to penetration is based on cavity expansion

expressions. We shall also compare our simulation results with his predictions for the specific cases tested here.

The purpose of the work presented here was to further investigate the process of secondary penetration using our 2D code. Our main motivation stems from the scarcity of data and analysis concerning this issue, as was clearly stated by Orphal [5]. He analyzed his ceramic penetration results using the above-mentioned secondary penetration models and concluded that the inverted rod mechanism suggested in [2], does not take place for the ceramic targets he used.

Numerical Simulations

All the simulations.in this work were performed with cylindrical rods, 8 mm in diameter, having 11 cells on their radius, in order to ensure numerical convergences (see [6]). The targets were large enough to be considered semi-infinite, both by their lateral dimensions and their thickness. This was achieved by adding FLOW boundary conditions to the central range of the targets, which were at least 30 rod diameters wide. Most of the simulations were performed with a simple von-Mises yield criterion for both the penetrator and target. Since we focus on very high impact velocities (up to 7 km/s), details of material failure are not important and the von-Mises criterion is enough to explore the penetration process. We should emphasize here that our simulations are not intended to match empirical data, but rather, result in the dependence of penetration depths on the relevant material parameters. As was clearly stated in [9] "in the long run large scale computing is the only method that can be expected to deal effectively with complex geometric shapes and new configurations........". It is our firm belief that even with relatively simple configurations, such as the normal impact of hypervelocity rods, one can gain a lot of understanding by using these codes, as we shall demonstrate here.

The output of our simulations was displayed through the time histories of several parameters. These included: penetration depth, rod length, rod-target interface pressure, and the velocities of the back and front ends of the rod. Figure 1 shows typical simulation results of these variables for a zero strength L/D=10 steel rod, impacting an 0.4 GPa aluminum target.

Several features of these time histories should be noted: 1) the steady-state nature of the penetration process for most of the time; 2) the abrupt breaks in velocities and interface pressure; and 3) the asymptotic behavior of the penetration depth, which is typical for the secondary penetration process as a result of the high velocity imparted to the bottom of the crater. Our simulations show that for impact velocities above 3 km/s, a two-stage penetration process is evident. The major issue at hand is to determine the exact time which marks the end of primary penetration and the start of secondary penetration. A close examination of many simulation results reveals the following order of the relevant times. The earliest time is at the end of the plateau in the velocity of the back end of the rod (V). Next, we find three very close events: the end of the plateau in the interface pressure, the break in the slope of rod length history and the end of the plateau in the penetration velocity (U). A few microseconds later, we find the break in the slope of the penetration-time history. All these events differ by 1 to 3 microseconds, in most cases. In order to have a consistent criterion for the transition between primary and secondary penetration, we chose the time at which the interface pressure history is dropping, since it occurs in the middle of the range described above and also because it is a very distinct and well-defined event. Moreover, the fact that the penetration velocity and the rod length histories have their breaks almost simultaneously, strongly enhances the choice of this event as the transition between primary and secondary penetrations.
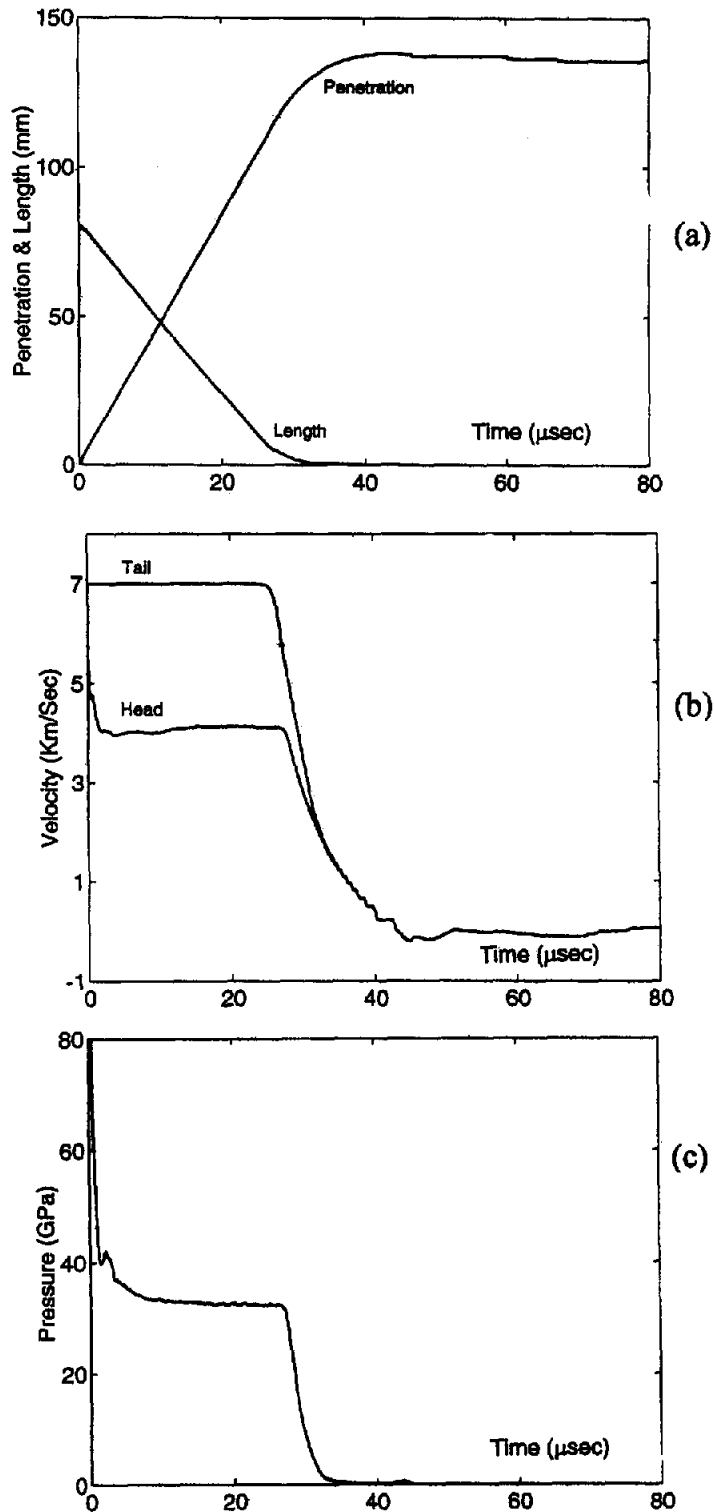
Fig. 1. Typical simulation results for time histories of: a) penetration velocity
and back-end velocity; b) rod length and penetration depth; and
c) interface-pressure at rod-target boundary.

Simulation Results

Zero Strength Rods. The first set of simulations was performed with zero strength steel rods impacting aluminum targets at 1-7 km/s. The use of zero strength rods avoids the complications arising from rod strength, enabling one to concentrate on the other parameters, such as rod and target density, target strength, etc. Figure 2 presents the data (normalized penetration vs. Impact velocity) for five steel rods, with aspect ratios in the range of 3-30, impacting an 0.4 GPa aluminum target. One can clearly see that the normalized penetration $P/\alpha L$ ($\alpha = \sqrt{\rho_P / \rho_t}$) is decreasing with increasing aspect ratio (L/D), as is well established by now. It is interesting to note, though, that this decreasing trend has an asymptotic nature and that for L/D > 25, or so, the normalized penetration tends to the hydrodynamic limit of 1.
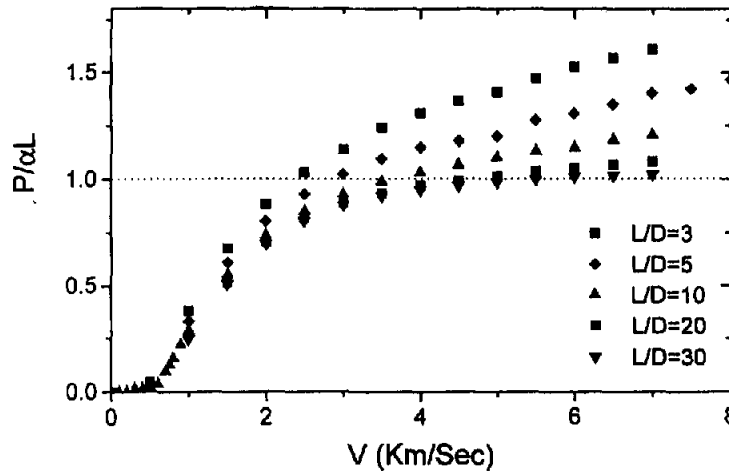

Fig. 2. Simulation results for zero strength steel rods impacting an 0.4 GPa aluminum target.

In order to compare our simulation results with the analytical models mentioned above, and, particularly, with that of Christman and Gehring [1], we consider their expression for the total penetration

$$P_{total} = P_h + P_{sec} = \left(\frac{\rho_P}{\rho_t}\right)^{1/2} (L - D) + 2.42 \cdot D \cdot \left(\frac{\rho_P}{\rho_t}\right)^{2/3} \cdot \left(\frac{\rho_t V^2}{B_{max}}\right)^{1/3} \qquad (1)$$

where B_{max} is the dynamic strength (hardness) of the target.

According to this model, the secondary penetration is achieved by the last segment of the rod having a length of about one diameter, while the main portion of the rod (of length L-D) is penetrating according to the simple hydrodynamic theory. Re-arranging Eq. (1) above, we find, for the normalized secondary penetration

$$\frac{P_{sec}}{\alpha \cdot D} = \frac{P_{total}}{\alpha D} - \left(\frac{L}{D} - 1\right) = 2.42 \cdot f(\rho_P, \rho_t) \cdot \left(\frac{V^2}{B_{max}}\right)^{1/3}. \qquad (2)$$

where f is the appropriate function of ρ_P and ρ_t. According to this expression, the secondary penetration should be proportional to $V^{2/3}$ and inversely proportional to $B_{max}^{1/3}$. Moreover, $P_{sec}/\alpha D$ should be the same for all L/D values, at a given impact velocity.

Figure 3 shows the simulation results from Figure 2, presented according to Eq. (2), for the high impact velocity range (3-7 km/s), where the secondary penetration is appreciable. One can clearly see that the simulation results do not fall on a single curve for all the different rods, in contrast with the prediction of Ref. [1], as manifested by Eq. (2). Furthermore, the dependence on impact velocity is very different for the five L/D values, as is evident in Figure 3. A least square fit of these simulations results in the following exponents for the velocity dependence of $P_{sec}/\alpha D$: 0.72, 1 and 1.8 for the L/D=3, 5 and 10, respectively. For the higher L/D values (20 and 30), the dependence of P_{sec} on V is more complicated. Thus, the $V^{2/3}$ dependence of P_{sec} is adequate only for the L/D=3 rods, according to our simulations.
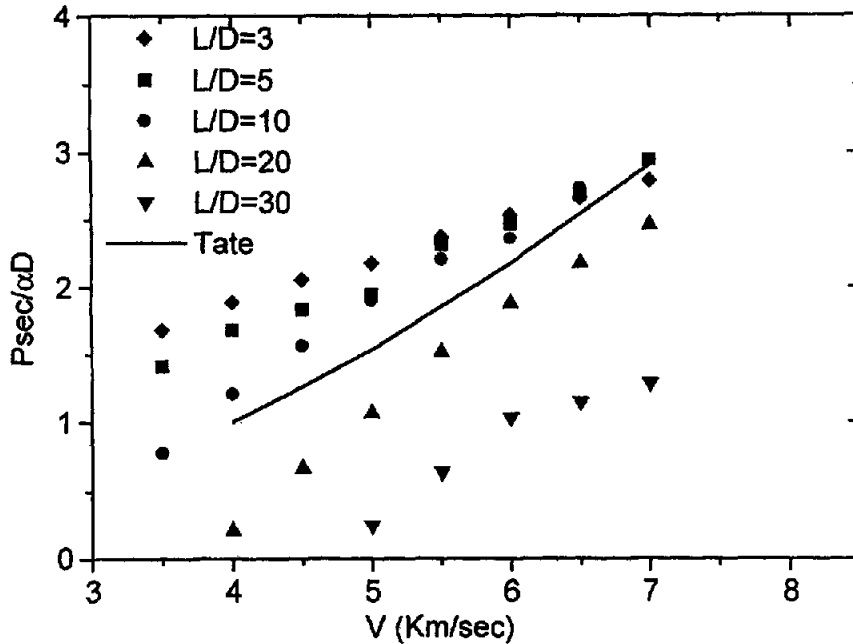

Fig. 3. The normalized secondary penetration extracted from the simulation results through Eq. (2). The line is Tate's model prediction [8].

Another model which has been proposed for the secondary penetration is that of Tate [8]. This model is based on two target resistance parameters R_t and R_{spt}, which are given by:

$$R_t = Y_t^d \left(\frac{2}{3} + \ell n \frac{0.57E}{Y_t^d} \right) \quad ; \quad R_{spt} = \frac{2}{3} Y_t^d \left(1 + \ell n \frac{2E}{3Y_t^d} \right) \tag{3}$$

where Y_t^d is the dynamic strength of the target and E is its Young's modulus.

Tate [8] recommended using an empirical value for Y_t^d through $Y_t^d = 4.2 \times (BHN)$, where BHN is the Brinell Hardness of the target.

These values of target resistance are inserted in the following equations to calculate P_{sec}:

$$\left(\frac{d_H}{D}\right)^2 = 1 + \frac{2\rho_P(V-U)^2}{R_t} \quad ; \quad \frac{P_{sec}}{d_H} = \frac{1}{4}\left[\left(1 + \frac{3\rho_t U^2}{2R_{spt}}\right)^{1/3} - 1\right] \tag{4}$$

where V and U are tail and head velocities of the rod and d_H and D are crater and rod diameters, respectively.

Using the nominal strength of the aluminum target (0.4 GPa), we obtain $R_t = 2.1$ GPa and $R_{spt} = 1.54$ GPa. These values were used to calculate $P_{sec}/\alpha D$ from Tate's model and compared with our simulation results in Figure 3. It is clearly evident that Tate's model is an excellent representation of the average simulation results. Considering the fact that this model does not predict an L/D dependence of P_{sec}, it is in good agreement with our results. This agreement is worse if we use a higher value of Y_t^d for the target strength.

Another way to compare our results with the model of Christman and Gehring is to actually plot the hydrodynamic and secondary parts of the total penetration. This is carried out in Figure 4 for L/D=5 and 20. The main point to consider here is the asymptotic values of the respective hydrodynamic parts. For the L/D=5, we obtain $P_{hyd}/\alpha L$ which converges to 0.8, while for L/D=20, the limit is 0.89. These values are in fair agreement with the basic claim of the model that the hydrodynamic penetration is achieved by the length of L-D, while the last segment (of length L≈D) is responsible for the secondary penetration. According to Eq. (1) for L/D=5 and 20, the hydrodynamic penetrations should converge to $P/\alpha L=0.8$ and 0.95, respectively. A similar analysis of our simulations for L/D=10 and 30 resulted in values of 0.85 and 0.92, respectively, which are also in fair agreement with those predicted by the model of [1] (0.9 for L/D=10, and 0.97 for L/D=30). Thus, we may conclude here that as far as the basic mechanism is concerned, the model of Christman and Gehring is verified by our simulations. The discrepancies lie in the detailed dependence of the secondary penetration on impact velocity for the different L/D rods.

Increasing Target Strength. Three more sets of simulations were performed with zero strength L/D=10 steel rods impacting aluminum targets with strengths of 0.8, 1.2 and 1.6 GPa. The results of these simulations are given in Figure 5. The following values were obtained for the secondary penetrations at 5, 6 and 7 km/s: for the 0.8 GPa target we find $P_{sec} = 23$, 27 and 33 mm, while for 1.2 GPa target $P_{sec} = 18$, 25 and 31 mm. For the 1.6 GPa target we obtained $P_{sec} = 18.6$, 20 and 23 mm. Here again, the P_{sec} values are nearly linear in velocity within each set, in contrast with the prediction of Ref. [1]. As for the strength dependence, we find for $V=7$ km/s, that the set of P_{sec} values (41.2, 33, 26 and 23 mm) are related by a $Y^{0.42}$ relationship better than by $Y^{1/3}$ (predicted in [1]). Thus, the combined strength-velocity dependence of the secondary penetration, according to our simulations, is closer to $V/Y^{1/2}$, rather than to $(V^2/Y)^{1/3}$ which is predicted by [1]. It is also interesting to note that even with the high strength target (1.6 GPa), the hydrodynamic penetration tends to $P/\alpha L=0.85$.
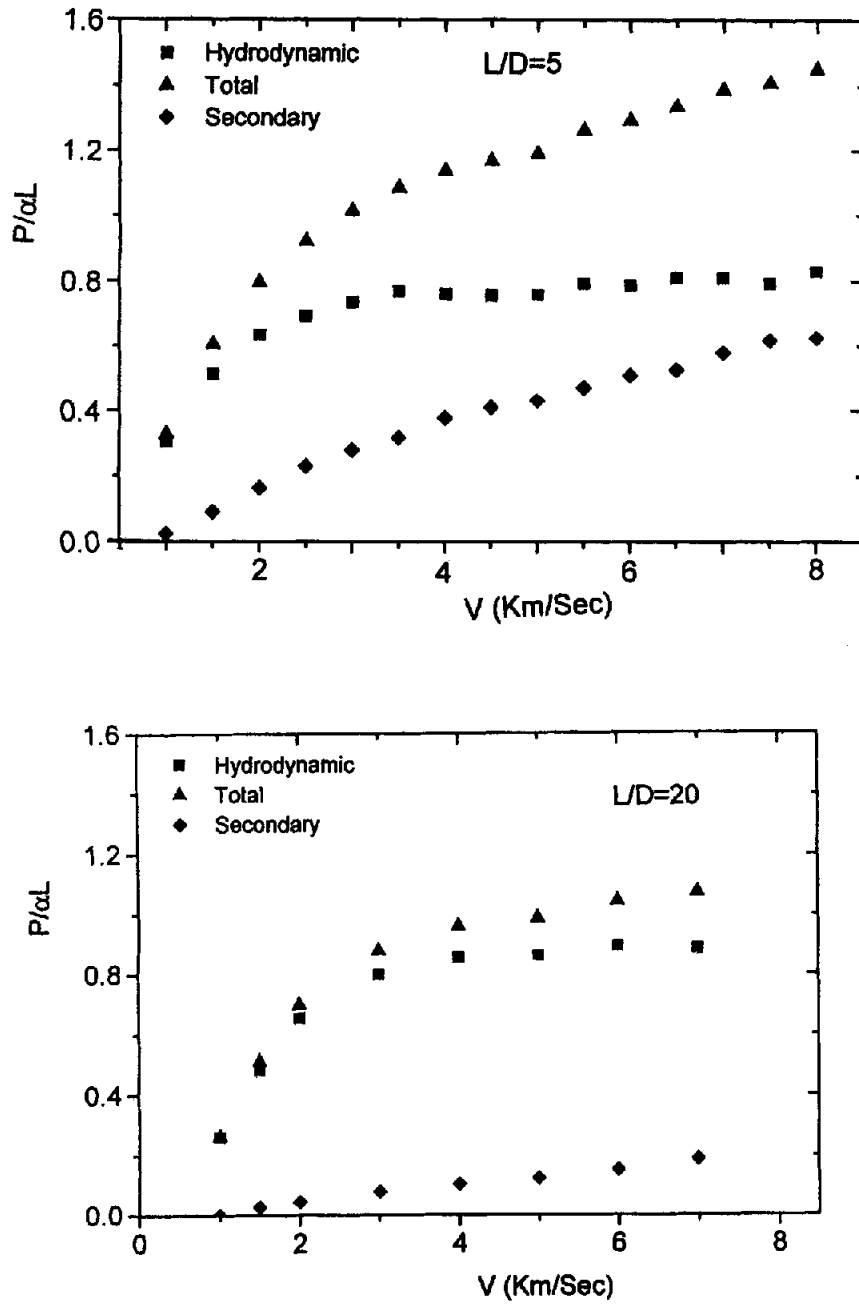
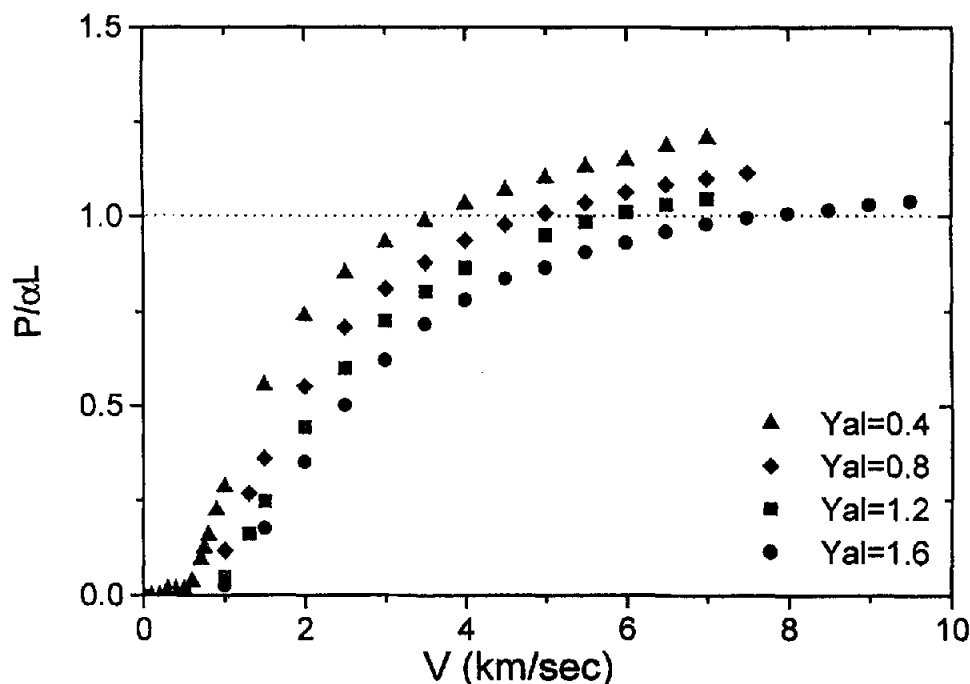Fig. 4. The results for hydrodynamic and secondary penetrations for L/D=5 and 20.

Fig. 5. Simulation results for L/D=10, zero strength steel rods, impacting aluminum targets with different strengths.

Returning to the model of Tate [8], we find that by using the simulation values of V and U for the 1.2 GPa target, we obtain P_{sec} = 9 and 15 mm for impact velocities of 5 and 6.5 km/s, respectively. These values are lower than those obtained by the simulations, according to the procedure described above, of 18 and 27 mm, for 5 and 6.5 km/s, respectively. Thus, as a general trend, the values predicted by Tate's model, for the strong targets, are lower by about 50% than those obtained by the simulations. We should note that a higher (dynamic) yield strength for the target would reduce these values even more and the agreement with the simulations would be worsened.

It is also worth noting that the values for primary penetrations in the three sets of simulations (with target strengths of 0.4, 0.8 and 1.2 GPa) are nearly equal for the velocity range of 5-7 km/s at about 117 mm. This amounts to a normalized penetration of P/αL=0.86 for the hydrodynamic part of penetration into the three different strength targets. As mentioned above, this value is in good agreement with the value of P/αL=0.9 for L/D=10 rods, which the model of Christman and Gehring [1] predicts for the hydrodynamic (primary) penetration.

Adding Strength to the Penetrator. In order to appreciate the effect of penetrator strength, we repeated the L/D = 10 steel rod simulations with strength ranging from 0-2.0 GPa. Figure 6 shows the results of these simulations.
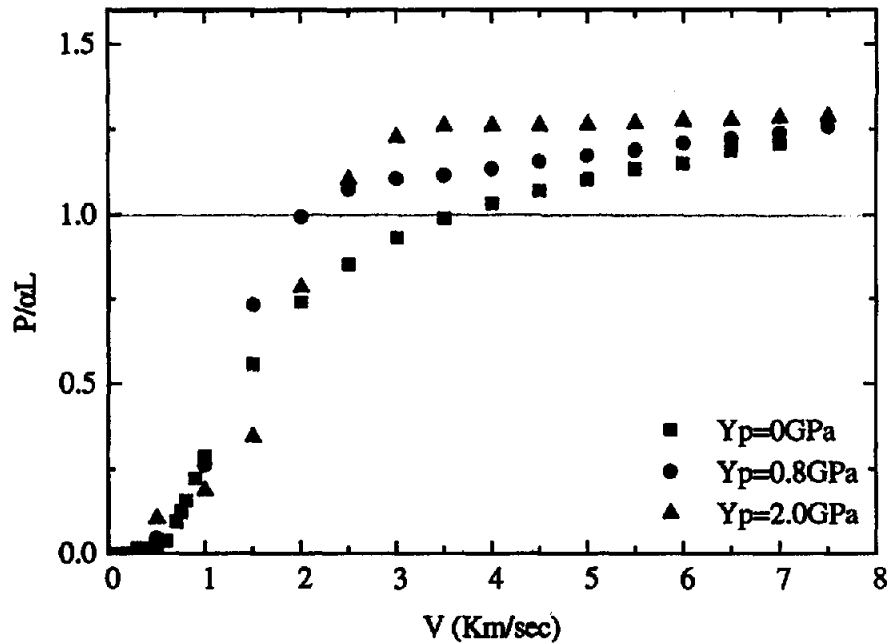
Fig. 6. The effect of penetrator strength on the normalized penetration of
L/D=10 steel rods impacting 0.4 GPa aluminum targets.

One can see the effect of penetrator strength on the final penetration depth, which is quite prominent even at the high velocity end (where it was always assumed that strength effects are negligible). The fact that rod strength plays an important role, even at high velocities, has been recently emphasized both by us in [6] and by Anderson et al [10]. The most interesting result of our simulation is that with increasing rod strength the penetration curves reach a shape of constant level with little (or no) dependence on impact velocity (for $Y_P = 2.0$ GPa). This, of course, is in total disagreement with the model of [1], which, as discussed above, suggests a $V^{2/3}$ dependence of the secondary penetration on velocity. One should emphasize the fact that the model in [1] (Eq. (1)) does not consider rod strength at all, which is probably the result of the relatively soft penetrators used by Christman and Gehring in their study. It is also interesting to note the apparent convergence of the three sets of results to a common value for $P/\alpha L$ at high impact velocities (near 7 km/s).

Another interesting feature is related to the hydrodynamic part of the penetration $P_{hyd}/\alpha L$, which increases with increasing rod strength. Thus, for 2.0 GPa rods, we find that $P_{hyd}/\alpha L$ reaches 0.86 for L/D=5, and is very nearly 1 for the L/D=20 and 30 rods. Since neither the model of Christman and Gehring [1], nor Tate's [8] include rod strength, we can only compare these trends with empirical data. Since these are usually given by the total depth of penetration, rather than by primary and secondary, we can only compare the general shape of our simulation results for high strength rods with those found in the published literature, as we show in Figure 7 data for tungsten alloy rods impacting aluminum (see [11]).
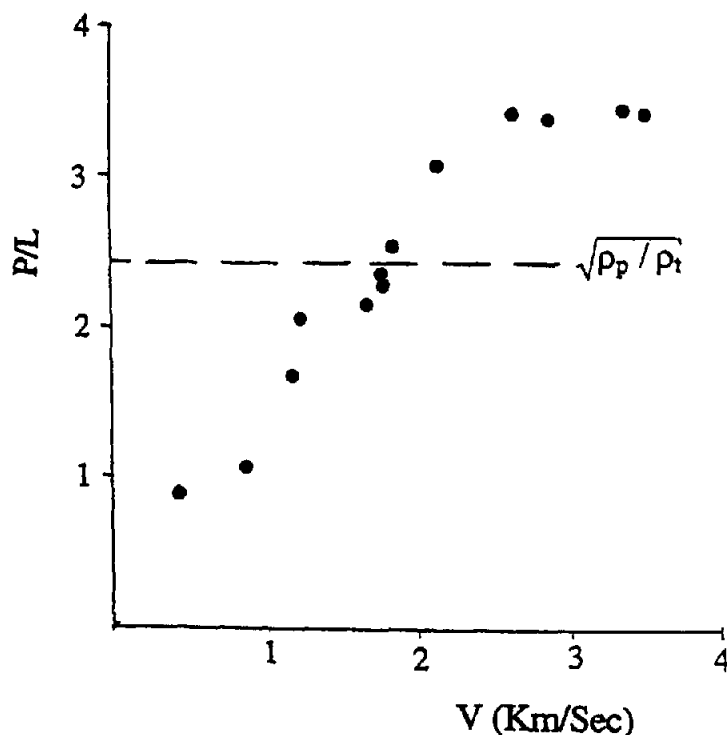
Fig. 7. The data for WA rods impacting aluminum targets (from [11]).

One can clearly see the excess constant penetration (above the hydrodynamic limit) which has been attributed by the authors of [11] to the secondary penetration mechanism suggested by Allen and Rogers [2]. With the results of our simulations, there is no reason to rely on this mechanism as we also explained in [6]. We have shown there that with strong gold penetrators (ρ_P = 19.3 g/cc, Y_P ≈ 1.2-2 GPa) and with 0.4 GPa aluminum targets, relatively high and constant $P/\alpha L$ are obtained, in good agreement with the results of Hohler and Stilp [11] for tungsten on aluminum. Thus, $P/\alpha L$ can reach values near 1.5 and even higher with strong and dense rods impacting relatively soft targets, without the mechanism of inverted rod penetration. Moreover, the penetration depths seem to be almost constant for a large velocity range, as our simulations predict.

The Effects of Rod Density. The final set of simulations was performed in order to find the sensitivity of secondary penetration to rod density. Except for the density, all the physical parameters of the rods remained the same as for the L/D = 10 steel rods. Two densities were chosen (ρ_P = 4.5, 15 g/cc) to represent the relevant range of rod densities encountered in the field. The strength of the rods was zero in order to avoid the extra effects caused by rod strength. The results of these simulations are shown in Figure 8, together with those for the steel rods (ρ_P = 7.83 g/cc). The most significant result is the fact that the three curves converge at the high velocity end. Thus, as far as $P/\alpha L$ is concerned, there is no difference between the three rods for velocities higher than about 5 km/s. At these impact velocities, if is quite clear that our results are in sharp contradiction with the model in [1], which asserts that the extra (secondary) penetration is strongly dependent on (ρ_P/ρ_t). Moreover, the fact that $P/\alpha L$ converges to a single curve for the three rod densities, also enhances our claim (in [6]), that the inverted rod mechanism, proposed by Allen and Rogers [2] for high density rods, is probably wrong.
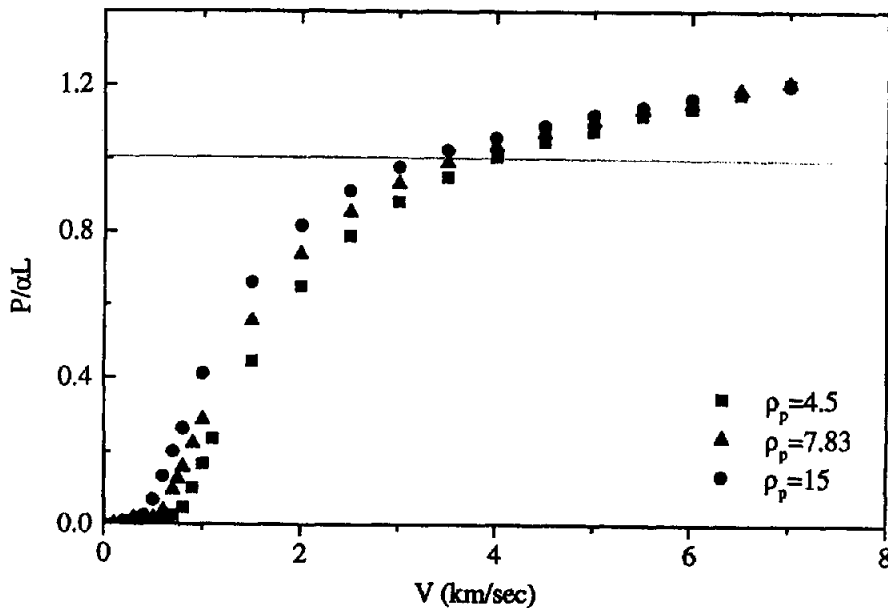
Fig. 8. Simulation results for rods of different densities (L/D=10) impacting 0.4 GPa targets.

CONCLUSIONS

The set of 2D numerical simulations, described in the present paper, was performed in order to gain some insight into the issue of secondary penetration of long rods. We find that the basic concept of Christman and Gehring [1], concerning the existence of a hydrodynamic (primary) penetration phase and later, velocity-dependent secondary phase, is correct, at least qualitatively. The details pertaining to the velocity dependence, rod/target density ratio, and influence of rod strength, are quite complicated. The model of Tate [8] is able to account for some of these details, especially the velocity dependence of the secondary penetration. However, other features are not reproduced by this model. Clearly the secondary penetration requires more investigation in order to successfully account for this process.

REFERENCES

[1]   Christman DR, Gehring WJ. *J. App. Phys.*, 1966; **37**, 1579.
[2]   Allen WA, Rogers JW. *J. Franklin Institute*, 1961; **272**, 275.
[3]   Bless SJ, Jurick D, Yoon B. *Proc. 9th Int. Symp. On Ballistics*, 1986; pp. 2-345.
[4]   Subramanian R, Bless SJ, Cazamias S, Berry D. *Int. J. Impact Eng.*, 1995; **17**, 817.
[5]   Orphal DL. *Int. J. Impact Eng.*, 1997; **20**, 601.
[6]   Rosenberg Z, Dekel E. *Int. J. Impact Eng.*, 2000; **24**, 85.
[7]   Cullis I, Nash. *Proc. 9th Int. Symp. On Ballistics*, 1986; pp. 2-351.
[8]   Tate A. *Int. J. Mech. Sci.*, 1986; **28**, 599.
[9]   Wright TW, Frank K. *BRL Technical Report*, 1988; BRL-TR-2957.
[10] Anderson Jr. CE, Orphal DL, Franzen RR, Walker JD. *Int. J. Impact Eng.*, 1999; **22**, 23.
[11] Hohler V, Stilp AJ. *5th Int. Symp. On Ballistics*, 16-18 April, 1980; Toulouse, France.